Report

ANIE: A mathematical algorithm for automated indexing of planar deformation features in quartz grains

Matthew S. HUBER[1*], Ludovic FERRIÈRE[2], Anna LOSIAK[1], and Christian KOEBERL[1,2]

[1]Department of Lithospheric Research, University of Vienna, Althanstrasse 14, A-1090 Vienna, Austria
[2]Natural History Museum, Burgring 7, A-1010 Vienna, Austria
*Corresponding author. E-mail: matthew.huber@univie.ac.at

Abstract–Planar deformation features (PDFs) in quartz, one of the most commonly used diagnostic indicators of shock metamorphism, are planes of amorphous material that follow crystallographic orientations, and can thus be distinguished from non-shock-induced fractures in quartz. The process of indexing data for PDFs from universal-stage measurements has traditionally been performed using a manual graphical method, a time-consuming process in which errors can easily be introduced. A mathematical method and computer algorithm, which we call the Automated Numerical Index Executor (ANIE) program for indexing PDFs, was produced, and is presented here. The ANIE program is more accurate and faster than the manual graphical determination of Miller–Bravais indices, as it allows control of the exact error used in the calculation and removal of human error from the process.

INTRODUCTION

The presence of planar deformation features (PDFs) in quartz grains has been used as one of the most reliable indicators of shock metamorphism for the confirmation of hypervelocity impact structures (see, e.g., French and Short 1968; Stöffler and Langenhorst 1994; Grieve et al. 1996; French 1998; French and Koeberl 2010 and references therein). PDFs have regularly spaced, thin, planar features generally oriented parallel to rational crystallographic planes (Fig. 1) and formed in quartz grains upon shock compression greater than approximately 5–10 GPa (see Stöffler and Langenhorst 1994 and references therein). As they develop along crystallographic planes, suspected planar features can be investigated (i.e., measured and indexed) to determine if they correspond to known planes that accommodate shock deformation (Engelhardt and Bertsch 1969; Stöffler and Langenhorst 1994; Ferrière et al. 2009). PDFs with specific crystallographic orientations are known to form in quartz at different shock pressures

(e.g., Hörz 1968; Müller and Défourneaux 1968; Huffman and Reimold 1996), so that peak shock pressure can be estimated for a given sample based on PDF orientations measurements (e.g., Robertson and Grieve 1977; Grieve et al. 1990; Dressler et al. 1998; Ferrière et al. 2008). The measurement of the orientations of suspected PDFs is possible using transmission electron microscopy (TEM; e.g., Goltrant et al. 1991; Trepmann and Spray 2006), a spindle stage (e.g., Bohor et al. 1987), or the universal-stage (U-stage) on a petrographic microscope (e.g., Engelhardt and Bertsch 1969; Langenhorst 2002; Ferrière et al. 2009). Nevertheless, a note of caution is necessary: determining if some planar features are true PDFs, especially if they are altered (e.g., in the form of planar fluid inclusion trails), is not possible based on only the determination of the crystallographic orientation of these features, because deformation of quartz crystals will often (but not exclusively) follow the rational crystallographic planes even if shock metamorphism is not involved. Thus, presentation of an orientation diagram alone is not
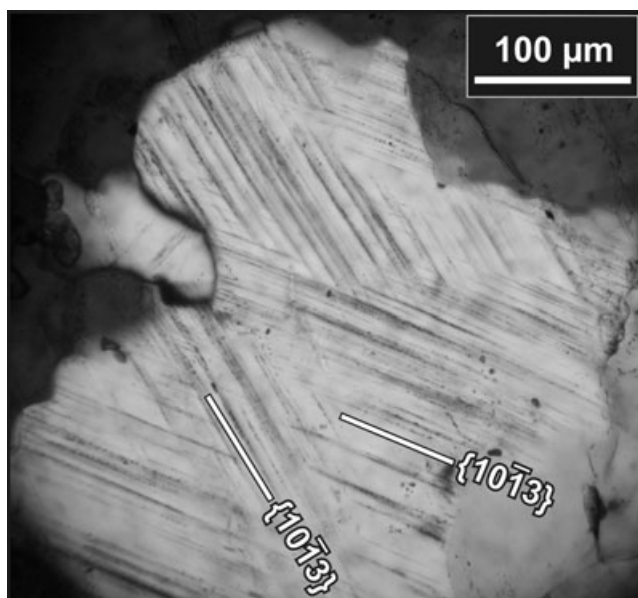
Fig. 1. Photomicrograph (crossed polars) of a quartz grain with two sets of planar deformation features (PDFs); both PDF sets with ω{10$\bar{1}$3}-equivalent orientations (sample from the Bosumtwi impact crater).

sufficient to confirm the presence of true PDFs. For such questionable features, TEM work remains necessary.

The most common and least expensive method of determining PDF orientations in quartz is the U-stage microscope analysis. According to the recent study by Ferrière et al. (2009), it is also the only technique that allows large, statistically significant data sets to be readily generated. However, the manual process of converting raw measurements from the U-stage to orientations of PDFs has traditionally been done using a graphical method based on a Wulff (equal-angle) stereonet and a stereographic projection template (see, e.g., Engelhardt and Bertsch 1969; Ferrière et al. 2009), and is rather time-consuming. It is also possible that manually determining the Miller–Bravais indices using the graphical method may introduce some additional errors to the data. Herein, for the first time, the mathematical basis for indexing PDFs is presented, along with an algorithm for indexing, named Automated Numerical Index Executor (ANIE), designed for use in Microsoft Excel (version 2007 and later). In addition, mathematically indexed PDFs from three samples, BOS (a meta-graywacke from the Bosumtwi impact crater), M8 (a biotite-gneiss from the Manson impact structure), and AUS (a sandstone from the Gosses Bluff impact structure) (see Ferrière et al. [2009] for more details on these samples) are compared with results obtained by the manual method (i.e., using the stereographic projection template) to demonstrate the veracity of our mathematical method.

MATHEMATICAL METHOD FOR DETERMINING CRYSTALLOGRAPHIC ORIENTATIONS OF PDFS

Previously, indexing PDFs has involved a graphical interface, as described in, e.g., Engelhardt and Bertsch (1969), Stöffler and Langenhorst (1994), and Ferrière et al. (2009). However, this method is, as mentioned above, time-consuming and somewhat imprecise, as it allows a certain "fudge factor" in the plotting of measurements on the stereonet, in the adjustment of the data, and in the actual reading of indices from the projected chart. All these inconveniences provided the motivation for a mathematical method to determine crystallographic orientations of PDFs.

The stereonet (or Wulff net) essentially represents a two-dimensional projection of a three-dimensional sphere. To determine PDF orientations using the stereonet, several steps must be followed. In the first step, the azimuth and inclination of the c-axis and poles perpendicular to planes of all PDFs in a given grain are plotted on a stereonet. Data are then adjusted by rotating the overlay by hand until the c-axis and a given pole lie on the same meridian (N-S great circle on the stereonet) to obtain the polar angle. Next, the c-axis is moved along the equatorial line of the stereonet to the center, and the poles perpendicular to planes of all PDFs are transformed along small circles by the same angle. Finally, the transformed data are compared with the stereographic projection template (STP) of PDFs in quartz, which displays the pole orientations of known PDF planes within a 5° envelope of measurement error. This last step is done by rotating the STP until all poles (or a maximum of them) fall into the circles of the STP (see, e.g., Engelhardt and Bertsch [1969]; Langenhorst [2002]; and/or Ferrière et al. [2009] for the detailed procedure). We describe here how all these graphical steps can be performed using mathematical calculations derived from spherical trigonometry (see Fig. 2).

The first step is to calculate the great circle distance between the c-axis and the pole to PDF plane, which corresponds to the so-called polar angle. This distance is obtained from the Law of Cosines for spherical triangles, and can be calculated using the following equation:

$$\cos(90 - \Psi) = \cos(90 - z) * \cos(90 - \Lambda) + \cos(90 - z)$$
$$* \cos(90 - \Lambda) * \cos(\alpha - a) \quad (1)$$

where "z" is the measured c-axis inclination, "α" is the measured c-axis azimuth, "Λ" is the measured PDF inclination, "a" is the measured PDF azimuth, and "Ψ" is the polar angle of the PDF. Note that the center of the sphere would be measured at 90°, so that it is necessary for calculations to be taken as "90 minus measurement" (see Fig. 2). Therefore, the equation can be simplified as follows:
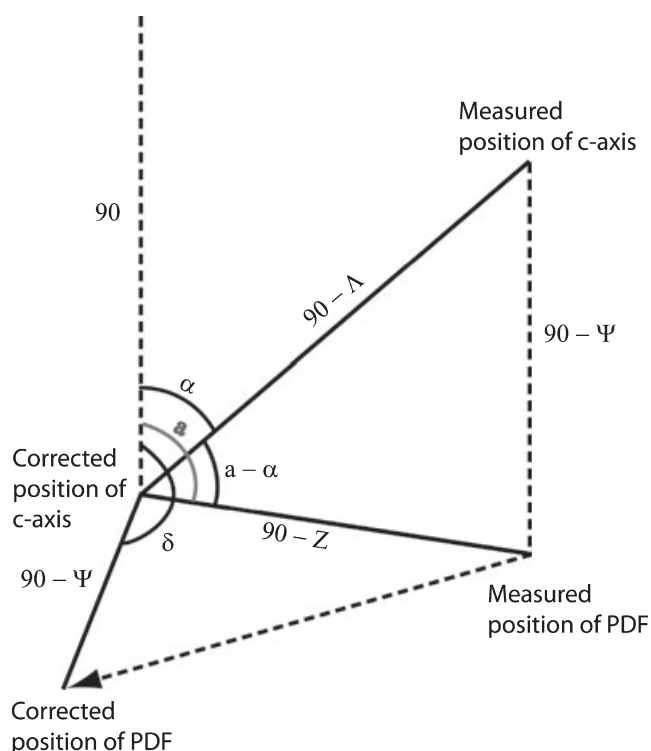
Fig. 2. Simplified representation of the process of indexing planar deformation features (PDFs) in quartz. The *c*-axis is measured, then moved to the center of a projected sphere; this operation is defined by a distance of "90−Λ" and an angle of "α." The distance between the center of the projected sphere and the measured position of the pole to PDF plane is "90−*z*," and the angle is "*a*." There is a distance of "90−Ψ" between the *c*-axis and the pole to PDF plane, which is constant before and after correction to the center. The pole to PDF plane is moved to a new position, which has an angle of "δ." The angle between the *c*-axis and the pole to PDF plane is "a−α."

$$\sin \Psi = \sin z * \sin \Lambda + \sin z * \sin \Lambda * \cos(\alpha - a) \quad (2)$$

Then, the second step is to calculate the azimuth of the PDF as it would be if the *c*-axis were in the middle of the sphere. This is calculated from the Law of Sines for spherical triangles using the following equation:

$$\sin \delta / \sin(90 - z) = \sin(\alpha - a) / \sin(90 - \Psi) \quad (3)$$

which simplifies to the following equation:

$$\sin \delta = \sin(\alpha - a) * \cos z / \cos \Psi \quad (4)$$

where "δ" is the azimuthal angle of the PDF after correcting the *c*-axis to the center of the sphere. Importantly, the value of "δ" must be corrected to determine the exact azimuth of the PDF, as this equation will only result in an accurate value for half of a circle (owing to the fact that cosine is an even function). To find the exact value of "δ," a determination of the proper quadrant is necessary. The value of "δ" does not

need adjustment if Equation 4 is positive and if sin (*z*) > sin (Ψ) × sin (Λ). The value of "δ" should be adjusted by "π−δ" if either Equation 4 is negative or sin (*z*) < sin (Ψ) × sin (Λ). In the case where Equation 4 is negative and sin (*z*) < sin (Ψ) × sin (Λ), the value of "δ" should be adjusted by "2π + δ" to ensure that "δ" refers to the correct quadrant and can be properly compared with other measured PDF sets in the given grain.

After the inclination "Ψ" and azimuth "δ" of all PDFs have been calculated for a given grain, the next step is to calculate the great circle distance between the two PDFs being indexed, "*c*"; this can be calculated using the following equation:

$$\cos c = \cos \Psi_1 * \cos \Psi_2 + \cos \Psi_1 * \cos \Psi_2 * \cos(\delta_1 - \delta_2) \quad (5)$$

Once this is calculated, the angle between PDFs (denoted here as "*C*") can be calculated using the Law of Cosines for spheres with the following equation:

$$\cos C = (\cos c - \cos \Psi_1 * \cos \Psi_2) / (\sin \Psi_1 * \sin \Psi_2) \quad (6)$$

The combination of the polar angle "Ψ" and the angle between PDF sets "*C*" allows PDFs to be indexed. Each PDF set has a singular polar angle and occurs at a particular angle to all other PDFs (see Table S1 in the Supporting Information). Two PDF sets can be indexed by first finding the polar angles close to the determined values, then determining if the angle between the measured planes "*C*" is within two times error (i.e., within the 5° envelope of measurement error for each PDF, or 10° error) to the angle between crystallographic planes in the grain.

DESCRIPTION OF THE AUTOMATED NUMERICAL INDEX EXECUTOR PROGRAM

Based on the mathematical method described above, a computer algorithm has been written as a Microsoft Excel 2007 macro. The program, named ANIE (see Supporting Information), allows the automated indexing of up to 10 PDF sets per grain in an unlimited number of quartz grains. Data can be entered directly as obtained from U-stage measurements, including input of the full range of values determined for a particular PDF set, which is input as the low and high measured values for both azimuth and inclination. Data can also be input as both East and West orientations.

From the input screen, the maximum error (corresponding to the "envelope of measurement error") that is traditionally fixed at 5° (see, e.g., Ferrière et al. 2009) can be defined by the user as any value between 0 and 10°. The user also has options concerning the method of calculation. Grains with a single PDF set can either be included or excluded from the analysis, and the program can either use an average value of the

U-stage measurements or the full range of measured values for indexing. When PDFs fall into the region where $\{10\bar{1}3\}$ and $\{10\bar{1}4\}$ orientations overlap, the program can be set to indicate that both orientations are possible solutions.

The measurements are matched to possible crystallographic indices based on the calculated polar angle (Equation 2) when compared with the ideal angle for each crystallographic index, plus or minus the defined error. Angles between ideal PDF sets (Equation 5) are compared with the list of possible angles between measured planes plus or minus the defined error (Table 1) to narrow the possible orientations for each plane to a single possible Miller–Bravais index. If there are multiple indices that are possible, the Miller–Bravais index with the lowest calculated angular error (i.e., the more likely) is reported.

Such analyses take only a few seconds to complete indexing for each grain; e.g., the analysis of sample AUS, with 208 PDF sets in 71 grains, was completed in approximately 1 minute. After the U-stage measurements are indexed, the program presents the results in two forms. The cumulative data are reported along with graphs presenting the proportion of indexed PDFs and the polar angles of the PDFs. The data are also presented in a grain-by-grain list, with details on the polar angle and Miller–Bravais indices of all PDF sets. Two histograms are presented upon completion of the program (Fig. 3); one with the frequency distribution of polar angle values in bins of 5°, and one with the absolute frequency of indexed PDFs with Miller–Bravais indices (see, e.g., Grieve et al. 1996; Ferrière et al. 2009). The number of PDF sets, the number of quartz grains, as well as the percentage of unindexed planes and the error used for the indexing, are indicated directly on the upper right part of the graph.

Data can also be exported to a comma-separated value spreadsheet, which retains the original input values, the polar angle values, the Miller–Bravais indices of the PDFs, and the angular error of the orientation for each PDF set in all grains. Graphics generated by the ANIE program can be exported directly to a Microsoft Powerpoint presentation, or they can also be copied for export to other programs.

COMPARISON OF MATHEMATICAL METHOD AND GRAPHICAL METHOD FOR INDEXING PDFS

The most recent stereographic projection template (with the pole orientations of known PDF planes; see Ferrière et al. 2009) used for the graphical method is designed to have 5° errors (i.e., "U-stage measurement errors") associated with all Miller–Bravais indices. However, additional errors can be introduced in this method from a number of factors, including the width of the line at the border of the circles (i.e., the 5° envelopes), the width of the pencil mark used when comparing the measurements to the STP by rotation, and the high likelihood that the human eye will not be able to properly discern whether measurements that are close to the border of a particular orientation are actually indexed or not. The mathematical method eliminates all of these factors of error and uncertainty. Due to that, a few minor discrepancies appear between the results obtained with graphical method versus mathematical method. Results are summarized in Table 1.

The data for three samples (AUS, BOS, and M8, all containing more than 65 grains with PDFs) have been processed mathematically using the ANIE program under four sets of conditions: (1) with a 5° error and using average values from U-stage data; (2) with a 5° error and using the full range from reported U-stage data; (3) with a 6° error and using average values from U-stage data; and (4) with a 6° error and using the full range from reported U-stage data. The reason for testing the mathematical method with a 6° error was to account for the potential "fudge factor" introduced by the graphical method. Note that all of the PDFs were indexed by hand with the graphical method by an experienced user (see Ferrière et al. 2009, for the exact methodology and procedure). Results using ANIE with average values from U-stage data with both 5° and 6° error have a noticeable difference compared with results obtained with the graphical method. However, very similar results are found between the graphical and mathematical results for 5° error using ranges of values, and near-identical results are found when 6° error is used with ranges of values.

Sample AUS is the largest data set indexed, with 74 grains and 208 measured PDF sets. By hand, it was found to have 10 unindexed planes, whereas when using ANIE and average values from U-stage data, with 5° and 6° error, 49 and 38 unindexed PDF sets were found, respectively. However, using the ranges of values resulted in 21 unindexed PDFs for 5° error, and 10 unindexed PDFs within 6° error. The graphically measured polar angles for AUS were similar to those found using ANIE, though with some minor discrepancies. For example, four PDFs were identified as being basal PDFs when plotted by hand, whereas they were unindexed using the mathematical method as the angular distance between the c-axis and the PDF set was slightly above error. The majority of differences between the graphical and mathematical method are the result of imprecision in the graphical method in the order of less than half a degree. Similar results were found for the samples BOS and M8 (Table 1).

Our comparison of results obtained with both methods allows us to identify three main categories of

Table 1. Comparison of the number of indexed planar deformation feature crystallographic orientations, as obtained using the graphical method and Automated Numerical Index Executor (ANIE) program with different settings, in quartz grains from three samples.

PDF crystallographic orientations	AUS sample (208 PDF sets in 74 grains)					BOS sample (145 PDF sets in 65 grains)					M8 sample (211 PDF sets in 71 grains)				
	Graphical method[a]	5° error averages[b]	5° error ranges[c]	6° error averages	6° error ranges	Graphical method	5° error averages	5° error ranges	6° error averages	6° error ranges	Graphical method	5° error averages	5° error ranges	6° error averages	6° error ranges
c (0001)	59	47	53	53	58	n.d.	n.d.	n.d.	n.d.	n.d.	4	4	4	4	4
$\{10\bar{1}4\}$[d]	6	8	22	6	21	2	12	13	7	12	10	7	17	4	14
$\{10\bar{1}4\}//\{10\bar{1}3\}$[e]	44	30	23	38	35	47	28	21	36	27	77	64	52	84	71
$\omega\{10\bar{1}3\}$[f]	60	48	59	48	53	32	34	45	35	42	79	61	78	56	65
$\pi\{10\bar{1}2\}$	2	2	3	2	3	28	23	28	27	29	2	2	6	2	6
$r, z\{10\bar{1}1\}$	10	11	12	10	12	5	7	7	6	8	13	10	15	14	16
$m\{10\bar{1}0\}$	1	1	3	1	3	1	1	1	1	1	n.d.	n.d.	n.d.	n.d.	n.d.
$\xi\{11\bar{2}2\}$	5	1	3	1	4	4	2	3	3	2	3	3	3	2	3
$s\{11\bar{2}1\}$	n.d.	n.d.	n.d.	n.d.	n.d.	2	2	4	3	4	n.d.	n.d.	1	1	1
$\rho\{21\bar{3}1\}$	3	3	4	2	4	3	2	2	3	2	3	3	8	3	8
$x\{51\bar{6}1\}$	1	2	2	2	2	1	1	n.d.	n.d.	n.d.	1	1	1	n.d.	1
$a\{11\bar{2}0\}$	1	1	n.d.	1	n.d.	1	n.d.	1	1	1	n.d.	n.d.	n.d.	n.d.	n.d.
$\{22\bar{4}1\}$	n.d.	n.d.	n.d.	n.d.	n.d.	6	5	3	5	3	10	9	6	12	6
$\{31\bar{4}1\}$	3	3	3	3	3	3	5	6	4	7	2	2	2	2	2
$t\{40\bar{4}1\}$	2	1	n.d.	1	n.d.	2	2	2	2	1	2	2	2	1	2
$k\{51\bar{6}0\}$	1	n.d.	n.d.	n.d.	n.d.	n.d.	n.d.	n.d.	n.d.	n.d.	1	1	n.d.	1	n.d.
Unindexed	10	49	21	38	10	8	21	9	12	6	5	42	16	25	12

[a] PDF planes indexed with the graphical method; Data from Ferrière et al. (2009).
[b] PDF planes indexed using ANIE program with a 5° envelope of measurement error and the average value of measurements for indexing.
[c] PDF planes indexed using ANIE program with a 5° envelope of measurement error and the ranges of values for indexing.
[d] $\{10\bar{1}4\}$ PDF orientations uniquely indexed.
[e] PDF planes which plot in the overlapping zone between $\{10\bar{1}4\}$ and $\{10\bar{1}3\}$ crystallographic orientations.
[f] $\{10\bar{1}3\}$ PDF orientations uniquely indexed.
n.d., none detected.

PDF Reference #	1	2	3	4	5	6	7	8	9	10	11	12	13	14	e	-	2+e
Miller-Bravais Indices	0001	1013	1012	1011	1010	1122	1121	2131	5161	1120	2241	3141	4041	5160	1014	Unindexed	1013+1014
Total Number of Sets	0	19	0	4	0	1	0	4	1	0	2	1	1	0	5	4	14
Absolute Frequency	0%	34%	0%	7%	0%	2%	0%	7%	2%	0%	4%	2%	2%	0%	9%	7%	27%
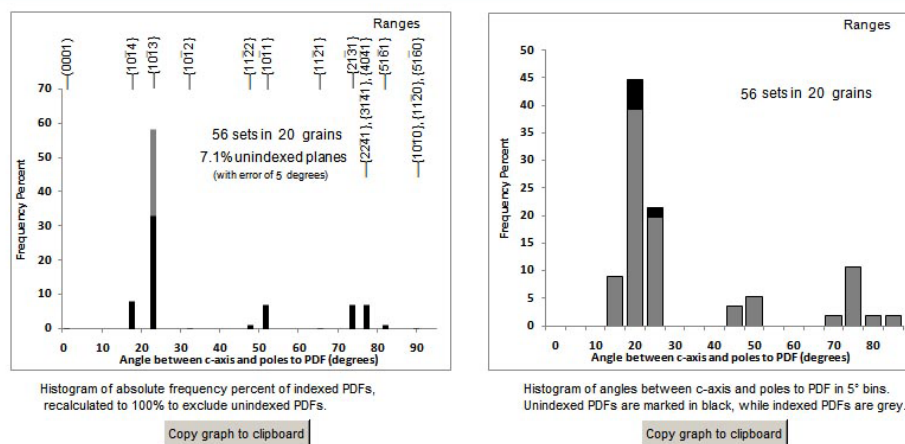
Fig. 3. Indexed planar deformation features (PDFs) data are summarized by the Automated Numerical Index Executor program as a pair of histograms, which show the absolute frequency percent of indexed PDFs and the frequency distribution of polar angle values of PDFs in 5° bins. The error used for analysis is indicated on the graph for indexed PDFs, and each graph also displays whether data are processed based on averages or ranges of values. Unindexed PDFs are marked in black on the histogram of polar angle values of PDFs.

differences between mathematical indexing using ANIE and the graphical indexing of the data. The first one arises when there are multiple possible solutions that allow all measurements to fit within known PDF crystallographic orientations. In the manual version, the user visually estimates the best fit (i.e., using eyes and "intuition"), whereas the mathematical method determines the set of Miller–Bravais indices that has the lowest error and, thus, is the most likely one. This accounts for 48% of the discrepancies. Secondly, PDF sets that are very close to a known PDF crystallographic orientation, but that fall just outside of the defined error (i.e., traditionally of 5° as in the STP presented in Ferrière et al. 2009) may be graphically counted as "indexed sets," even they are in fact unindexed PDFs. This also accounts for 48% of discrepancies. Finally, all other discrepancies between graphical versus mathematical method that do not correspond to either of these, such as errors in plotting data, account for the remaining 4% of discrepancies. The paucity of such discrepancies indicates that the mathematical method is reliably measuring the exact same features as when using the graphical method, whereas the commonality of the second category of discrepancies indicates that the user, in the case of the graphical method, can easily introduce some errors into the indexing process.

Thus, based on our comparison of results as obtained for the same set of U-stage data with the graphical method and the mathematical method (i.e., using ANIE), very similar results are obtained when using the range of measured values and an error of 6°. It is recommended that users of the ANIE program, or of the mathematical method described in this article, state specifically which error setting is chosen for the indexing of the PDFs and whether average values or ranges of values are used for the determination of crystallographic indices.

CONCLUSIONS AND RECOMMENDATIONS

The process of indexing PDFs in quartz grains is somewhat tedious, mainly because of the time-consuming and difficult nature of plotting U-stage measurements and properly reading the Miller–Bravais indices after the data have been obtained. The development and presentation of an automated method for the determination of crystallographic orientations of PDFs remove a large part of the tedium for those who are attempting to verify the shock origin of deformation features in quartz grains and/or who are interested in the evaluation of the peak shock pressure recorded by a given sample.

Our comparison of indexing PDF sets using the mathematical method (i.e., the ANIE program) versus the "old" graphical method reveals that the best fit between the two methods is found when using 6° error and the full ranges of values (as opposed to the average value of measurements) in the ANIE program. For the 564 PDFs evaluated in this study, a total of 46 differences were found between indexing with the mathematical method versus the graphical method, which corresponds

to a difference of about 8%. Finally, our study suggests that the graphical method, although designed with a 5° envelope of measurement error, is actually closer to 6° error in reality. However, it is recommended to users to define a 5° error when using ANIE program, because if a 6° error is used, the error envelopes of the PDFs pole traces for $\{10\bar{1}2\}$ and $\{10\bar{1}3\}$ orientations partially overlap. Anyone presenting PDF data indexed with the ANIE program or this mathematical method is asked to state clearly the error used in the calculation, as well as whether the average value of measurements or the ranges of values is used for indexing.

Editorial Handling— Dr. John Spray

REFERENCES

Bohor B. F., Modreski P. J., and Foord E. E. 1987. Shocked quartz in the Cretaceous-Tertiary boundary clays: Evidence for a global distribution. *Science* 236:705–708.

Dressler B. O., Sharpton V. L., and Schuraytz B. C. 1998. Shock metamorphism and shock barometry at a complex impact structure: State Islands, Canada. *Contributions to Mineralogy and Petrology* 130:275–287.

Engelhardt W. V. and Bertsch W. 1969. Shock induced planar deformation structures in quartz from the Ries crater, Germany. *Contributions to Mineralogy and Petrology* 20:203–234.

Ferrière L., Koeberl C., Ivanov B. A., and Reimold W. U. 2008. Shock metamorphism of Bosumtwi impact crater rocks, shock attenuation, and uplift formation. *Science* 322:1678–1681.

Ferrière L., Morrow J. R., Amgaa T., and Koeberl C. 2009. Systematic study of universal-stage measurements of planar deformation features in shocked quartz: Implications for statistical significance and representation of results. *Meteoritics & Planetary Science* 44:925–940.

French B. M. 1998. Traces of catastrophe: A handbook of shock-metamorphic effects in terrestrial meteorite impact structures. LPI Contribution 954. Houston, Texas: Lunar and Planetary Institute. 120 p.

French B. M. and Koeberl C. 2010. The convincing identification of terrestrial meteorite impact structures: What works, what doesn't, and why. *Earth-Science Reviews* 98:123–170.

French B. M. and Short N. M., eds. 1968. *Shock metamorphism of natural materials*. Baltimore: Mono Book Corporation. 644 p.

Goltrant O., Cordier P., and Doukhan J.-C. 1991. Planar deformation features in shocked quartz; a transmission electron microscopy investigation. *Earth and Planetary Science Letters* 106:103–115.

Grieve R. A. F., Coderre J. M., Robertson P. B., and Alexopoulos J. 1990. Microscopic planar deformation features in quartz of the Vredefort structure: Anomalous but still suggestive of an impact origin. *Tectonophysics* 171:185–200.

Grieve R. A. F., Langenhorst F., and Stöffler D. 1996. Shock metamorphism of quartz in nature and experiment: II. Significance in geoscience. *Meteoritics & Planetary Science* 31:6–35.

Hörz F. 1968. Statistical measurements of deformation structures and refractive indices in experimentally shock loaded quartz. In *Shock metamorphism of natural materials*, edited by French B. M. and Short N. M. Baltimore: Mono Book Corp. pp. 243–253.

Huffman A. R. and Reimold W. U. 1996. Experimental constraints on shock-induced microstructures in naturally deformed silicates. *Tectonophysics* 256:165–217.

Langenhorst F. 2002. Shock metamorphism of some minerals: Basic introduction and microstructural observations. *Bulletin of the Czech Geological Survey* 77:265–282.

Müller W. F. and Défourneaux M. 1968. Deformationsstrukturen im Quarz als Indikator für Stosswellen: Eine experimentelle Untersuchung an Quarz-Einkristallen. *Zeitschrift für Geophysik* 34:483–504.

Robertson P. B. and Grieve R. A. F. 1977. Shock attenuation at terrestrial impact structures. In *Impact and explosion cratering*, edited by Roddy D. J., Pepin R. O., and Merrill R. B. New York: Pergamon Press. pp. 687–702.

Stöffler D. and Langenhorst F. 1994. Shock metamorphism of quartz in nature and experiment: I. Basic observation and theory. *Meteoritics & Planetary Science* 29:155–181.

Trepmann C. A. and Spray J. G. 2006. Shock-induced crystal-plastic deformation and post-shock annealing of quartz: Microstructural evidence from crystalline target rocks of the Charlevoix impact structure, Canada. *European Journal of Mineralogy* 18:161–173.

SUPPORTING INFORMATION

Additional supporting information may be found in the online version of this article:

Table S1. Angular relationships between pairs of Miller–Bravais indices.

Program. Automated Numerical Index Executor. Requires Microsoft Excel 2007 or later.

Please note: Wiley-Blackwell is not responsible for the content or functionality of any supporting materials supplied by the authors. Any queries (other than missing material) should be directed to the corresponding author for the article.